

Observation of $X(3872)$ in $B \rightarrow X(3872)K\pi$ decays

A. Bala,⁴⁹ V. Bhardwaj,⁴⁰ K. Trabelsi,^{14,10} J. B. Singh,⁴⁹ A. Abdesselam,⁵⁸ I. Adachi,^{14,10} H. Aihara,⁶³ K. Arinstein,⁴ D. M. Asner,⁴⁸ V. Aulchenko,⁴ T. Aushev,^{37,23} R. Ayad,⁵⁸ T. Aziz,⁵⁹ S. Bahinipati,¹⁶ A. M. Bakich,⁵⁷ V. Bansal,⁴⁸ E. Barberio,³⁵ B. Bhuyan,¹⁷ A. Bobrov,⁴ G. Bonvicini,⁶⁸ A. Bozek,⁴⁴ M. Bračko,^{33,24} T. E. Browder,¹³ D. Červenký,⁵ A. Chen,⁴¹ B. G. Cheon,¹² R. Chistov,²³ K. Cho,²⁸ V. Chobanova,³⁴ S.-K. Choi,¹¹ Y. Choi,⁵⁶ D. Cinabro,⁶⁸ J. Dalseno,^{34,60} J. Dingfelder,³ Z. Doležal,⁵ A. Drutskoy,^{23,36} D. Dutta,¹⁷ S. Eidelman,⁴ D. Epifanov,⁶³ H. Farhat,⁶⁸ J. E. Fast,⁴⁸ T. Ferber,⁷ O. Frost,⁷ V. Gaur,⁵⁹ N. Gabyshev,⁴ A. Garmash,⁴ D. Getzkow,⁸ Y. M. Goh,¹² B. Golob,^{32,24} O. Grzymkowska,⁴⁴ J. Haba,^{14,10} T. Hara,^{14,10} H. Hayashii,⁴⁰ X. H. He,⁵⁰ A. Heller,²⁶ T. Horiguchi,⁶² W.-S. Hou,⁴³ M. Huschle,²⁶ T. Iijima,^{39,38} A. Ishikawa,⁶² R. Itoh,^{14,10} Y. Iwasaki,¹⁴ I. Jaegle,¹³ D. Joffe,²⁷ K. H. Kang,³⁰ E. Kato,⁶² T. Kawasaki,⁴⁶ C. Kiesling,³⁴ D. Y. Kim,⁵⁵ J. B. Kim,²⁹ J. H. Kim,²⁸ K. T. Kim,²⁹ M. J. Kim,³⁰ S. H. Kim,¹² Y. J. Kim,²⁸ K. Kinoshita,⁶ B. R. Ko,²⁹ P. Kodyš,⁵ S. Korpar,^{33,24} P. Križan,^{32,24} P. Krokovny,⁴ T. Kuhr,²⁶ R. Kumar,⁵² A. Kuzmin,⁴ Y.-J. Kwon,⁷⁰ J. S. Lange,⁸ I. S. Lee,¹² Y. Li,⁶⁷ L. Li Gioi,³⁴ J. Libby,¹⁸ D. Liventsev,⁶⁷ P. Lukin,⁴ D. Matvienko,⁴ K. Miyabayashi,⁴⁰ H. Miyake,^{14,10} H. Miyata,⁴⁶ R. Mizuk,^{23,36} G. B. Mohanty,⁵⁹ S. Mohanty,^{59,66} A. Moll,^{34,60} H. K. Moon,²⁹ R. Mussa,²² E. Nakano,⁴⁷ M. Nakao,^{14,10} Z. Natkaniec,⁴⁴ M. Nayak,¹⁸ N. K. Nisar,⁵⁹ S. Nishida,^{14,10} S. Ogawa,⁶¹ S. Okuno,²⁵ S. L. Olsen,⁵⁴ P. Pakhlov,^{23,36} G. Pakhlova,²³ C. W. Park,⁵⁶ H. Park,³⁰ R. Pestotnik,²⁴ M. Petrič,²⁴ L. E. Piilonen,⁶⁷ E. Ríbežl,²⁴ M. Ritter,³⁴ Y. Sakai,^{14,10} S. Sandilya,⁵⁹ L. Santelj,¹⁴ T. Sanuki,⁶² V. Savinov,⁵¹ O. Schneider,³¹ G. Schnell,^{1,15} C. Schwanda,²⁰ K. Senyo,⁶⁹ O. Seon,³⁸ M. E. Sevier,³⁵ V. Shebalin,⁴ C. P. Shen,² T.-A. Shibata,⁶⁴ J.-G. Shiu,⁴³ B. Shwartz,⁴ A. Sibidanov,⁵⁷ F. Simon,^{34,60} Y.-S. Sohn,⁷⁰ A. Sokolov,²¹ E. Solovieva,²³ M. Starič,²⁴ M. Steder,⁷ M. Sumihama,⁹ T. Sumiyoshi,⁶⁵ K. Tanida,⁵⁴ G. Tatishvili,⁴⁸ Y. Teramoto,⁴⁷ F. Thorne,²⁰ V. Trusov,²⁶ M. Uchida,⁶⁴ S. Uehara,^{14,10} T. Uglov,^{23,37} Y. Unno,¹² S. Uno,^{14,10} P. Urquijo,³⁵ Y. Usov,⁴ P. Vanhoefer,³⁴ G. Varner,¹³ A. Vinokurova,⁴ V. Vorobyev,⁴ M. N. Wagner,⁸ C. H. Wang,⁴² X. L. Wang,⁶⁷ Y. Watanabe,²⁵ K. M. Williams,⁶⁷ E. Won,²⁹ H. Yamamoto,⁶² Y. Yamashita,⁴⁵ S. Yashchenko,⁷ C. Z. Yuan,¹⁹ Z. P. Zhang,⁵³ V. Zhilich,⁴ V. Zhulanov,⁴ M. Ziegler,²⁶ and A. Zupanc²⁴

(Belle Collaboration)

¹University of the Basque Country UPV/EHU, 48080 Bilbao²Beihang University, Beijing 100191³University of Bonn, 53115 Bonn⁴Budker Institute of Nuclear Physics SB RAS and Novosibirsk State University, Novosibirsk 630090⁵Faculty of Mathematics and Physics, Charles University, 121 16 Prague⁶University of Cincinnati, Cincinnati, Ohio 45221⁷Deutsches Elektronen-Synchrotron, 22607 Hamburg⁸Justus-Liebig-Universität Gießen, 35392 Gießen⁹Gifu University, Gifu 501-1193¹⁰The Graduate University for Advanced Studies, Hayama 240-0193¹¹Gyeongsang National University, Chinju 660-701¹²Hanyang University, Seoul 133-791¹³University of Hawaii, Honolulu, Hawaii 96822¹⁴High Energy Accelerator Research Organization (KEK), Tsukuba 305-0801¹⁵IKERBASQUE, Basque Foundation for Science, 48013 Bilbao¹⁶Indian Institute of Technology Bhubaneswar, Satya Nagar 751007¹⁷Indian Institute of Technology Guwahati, Assam 781039¹⁸Indian Institute of Technology Madras, Chennai 600036¹⁹Institute of High Energy Physics, Chinese Academy of Sciences, Beijing 100049²⁰Institute of High Energy Physics, Vienna 1050²¹Institute for High Energy Physics, Protvino 142281²²INFN—Sezione di Torino, 10125 Torino²³Institute for Theoretical and Experimental Physics, Moscow 117218²⁴J. Stefan Institute, 1000 Ljubljana²⁵Kanagawa University, Yokohama 221-8686²⁶Institut für Experimentelle Kernphysik, Karlsruher Institut für Technologie, 76131 Karlsruhe²⁷Kennesaw State University, Kennesaw, Georgia 30144²⁸Korea Institute of Science and Technology Information, Daejeon 305-806²⁹Korea University, Seoul 136-713³⁰Kyungpook National University, Daegu 702-701³¹École Polytechnique Fédérale de Lausanne (EPFL), Lausanne 1015³²Faculty of Mathematics and Physics, University of Ljubljana, 1000 Ljubljana³³University of Maribor, 2000 Maribor

- ³⁴Max-Planck-Institut für Physik, 80805 München
³⁵School of Physics, University of Melbourne, Victoria 3010
³⁶Moscow Physical Engineering Institute, Moscow 115409
³⁷Moscow Institute of Physics and Technology, Moscow Region 141700
³⁸Graduate School of Science, Nagoya University, Nagoya 464-8602
³⁹Kobayashi-Maskawa Institute, Nagoya University, Nagoya 464-8602
⁴⁰Nara Women's University, Nara 630-8506
⁴¹National Central University, Chung-li 32054
⁴²National United University, Miao Li 36003
⁴³Department of Physics, National Taiwan University, Taipei 10617
⁴⁴H. Niewodniczanski Institute of Nuclear Physics, Krakow 31-342
⁴⁵Nippon Dental University, Niigata 951-8580
⁴⁶Niigata University, Niigata 950-2181
⁴⁷Osaka City University, Osaka 558-8585
⁴⁸Pacific Northwest National Laboratory, Richland, Washington 99352
⁴⁹Panjab University, Chandigarh 160014
⁵⁰Peking University, Beijing 100871
⁵¹University of Pittsburgh, Pittsburgh, Pennsylvania 15260
⁵²Punjab Agricultural University, Ludhiana 141004
⁵³University of Science and Technology of China, Hefei 230026
⁵⁴Seoul National University, Seoul 151-742
⁵⁵Soongsil University, Seoul 156-743
⁵⁶Sungkyunkwan University, Suwon 440-746
⁵⁷School of Physics, University of Sydney, New South Wales 2006
⁵⁸Department of Physics, Faculty of Science, University of Tabuk, Tabuk 71451
⁵⁹Tata Institute of Fundamental Research, Mumbai 400005
⁶⁰Excellence Cluster Universe, Technische Universität München, 85748 Garching
⁶¹Toho University, Funabashi 274-8510
⁶²Tohoku University, Sendai 980-8578
⁶³Department of Physics, University of Tokyo, Tokyo 113-0033
⁶⁴Tokyo Institute of Technology, Tokyo 152-8550
⁶⁵Tokyo Metropolitan University, Tokyo 192-0397
⁶⁶Utkal University, Bhubaneswar 751004
⁶⁷CNP, Virginia Polytechnic Institute and State University, Blacksburg, Virginia 24061
⁶⁸Wayne State University, Detroit, Michigan 48202
⁶⁹Yamagata University, Yamagata 990-8560
⁷⁰Yonsei University, Seoul 120-749

(Received 27 January 2015; published 2 March 2015)

We report the first observation of $B^0 \rightarrow X(3872)(K^+\pi^-)$ and evidence for $B^+ \rightarrow X(3872)(K^0\pi^+)$. We measure the product of branching fractions for the former to be $\mathcal{B}(B^0 \rightarrow X(3872)(K^+\pi^-)) \times \mathcal{B}(X(3872) \rightarrow J/\psi\pi^+\pi^-) = (7.9 \pm 1.3(\text{stat}) \pm 0.4(\text{syst})) \times 10^{-6}$ and find that $B^0 \rightarrow X(3872)K^*(892)^0$ does not dominate the $B^0 \rightarrow X(3872)K^+\pi^-$ decay mode. We also measure $\mathcal{B}(B^+ \rightarrow X(3872)(K^0\pi^+)) \times \mathcal{B}(X(3872) \rightarrow J/\psi\pi^+\pi^-) = (10.6 \pm 3.0(\text{stat}) \pm 0.9(\text{syst})) \times 10^{-6}$. This study is based on the full data sample of 711 fb^{-1} ($772 \times 10^6 B\bar{B}$ pairs) collected at the $\Upsilon(4S)$ resonance with the Belle detector at the KEKB collider.

DOI: [10.1103/PhysRevD.91.051101](https://doi.org/10.1103/PhysRevD.91.051101)

PACS numbers: 14.40.Pq, 12.39.Mk, 13.20.He

About a decade ago, the Belle Collaboration discovered the $X(3872)$ state [1] in the exclusive reconstruction of $B^+ \rightarrow X(3872)(\rightarrow J/\psi\pi^+\pi^-)K^+$ [2]. Considerable effort by both experimentalists and theorists has been invested to clarify its nature. As a result, we know precisely its mass (3871.69 ± 0.17) MeV/ c^2 [3], have a stringent limit on its width (less than 1.2 MeV at 90% confidence level) [4] and have a definitive J^{PC} assignment of 1^{++} [5]. The $X(3872)$ has been observed to decay to several other final states:

$J/\psi\gamma$ [6], $\psi'\gamma$ [7], $J/\psi\pi^+\pi^-\pi^0$ [8] and $D^0\bar{D}^{*0}$ [9,10]. The proximity of its mass to the $D^0\bar{D}^{*0}$ threshold, along with its measured partial decay rates, suggests that it be a loosely bound “molecule” of D^0 and \bar{D}^{*0} mesons [11] or an admixture of $D^0\bar{D}^{*0}$ with a charmonium ($c\bar{c}$) state [11,12]. Some authors have advanced a QCD-tetraquark interpretation for the $X(3872)$, and predict the existence of charged- and C-odd partner states that are nearby in mass [13]. Experimental searches for charged-[4,14] and C-odd

[15,16] partners report negative results. However, since these searches are restricted to states with narrow total widths, the published limits may not apply if the partner states access more decay channels and are thus broader. More experimental information on the production and decays of the $X(3872)$ will shed additional light on its nature.

In this paper, we present the results of searches for $X(3872)$ production via the $B^0 \rightarrow X(3872)K^+\pi^-$ and $B^+ \rightarrow X(3872)K_S^0\pi^+$ decay modes, where the $X(3872)$ decays to $J/\psi\pi^+\pi^-$. The study is based on 711 fb^{-1} of data containing $772 \times 10^6 B\bar{B}$ events collected with the Belle detector [17] at the KEKB e^+e^- asymmetric-energy collider [18] operating at the $\Upsilon(4S)$ resonance. In addition to selecting $B \rightarrow X(3872)K\pi$ signal events, the same selection criteria isolate a rather pure sample of $B \rightarrow \psi' K\pi$ events that are used for calibration.

The Belle detector is a large solid-angle magnetic spectrometer that consists of a silicon vertex detector (SVD), a 50-layer central drift chamber (CDC), an array of aerogel threshold Cherenkov counters (ACC), a barrel-like arrangement of time-of-flight scintillation counters (TOF), and an electromagnetic calorimeter (ECL) composed of CsI(Tl) crystals. All these detector components are located inside a superconducting solenoid coil that provides a 1.5 T magnetic field. An iron flux return located outside the coil is instrumented to detect K_L^0 mesons and to identify muons (KLM). The detector is described in detail elsewhere [17].

Monte Carlo (MC) samples are generated for each decay mode using EvtGen [19], and radiative effects are taken into account using the PHOTOS [20] package. The detector response is simulated using GEANT3 [21].

Charged tracks are required to originate from the interaction point (IP). To identify charged kaons and pions, we use a likelihood ratio $\mathcal{R}_{K/\pi} = \mathcal{L}_K / (\mathcal{L}_\pi + \mathcal{L}_K)$, where the kaon (pion) likelihood \mathcal{L}_K (\mathcal{L}_π) is calculated using ACC, TOF and CDC measurements. For the prompt charged kaon (pion), we apply the criterion $\mathcal{R}_{K/\pi}(\mathcal{R}_{\pi/K}) > 0.6$. Here, the kaon (pion) identification efficiency is 93% (95%) while the probability of misidentifying a pion as a kaon (kaon as a pion) is 8% (7%). For the pion daughters from ψ' or $X(3872)$, we impose $\mathcal{R}_{\pi/K} > 0.4$; the corresponding pion identification efficiency is 99% and the misidentification probability is 8%. Candidates for the $K_S^0 \rightarrow \pi^+\pi^-$ decay are formed from pairs of oppositely charged tracks having an invariant mass between 488 and $506 \text{ MeV}/c^2$ ($\pm 4\sigma$ around the nominal mass of K_S^0). The K_S^0 candidate is also required to satisfy the criteria described in Ref. [22] to ensure that its decay vertex is displaced from the IP. A track is identified as a muon if its muon likelihood ratio is greater than 0.1, where the muon and hadron likelihoods are calculated by the track penetration depth and hit scatter in the muon detector (KLM).

An electron track is identified with an electron likelihood greater than 0.01, where the electron likelihood is calculated by combining dE/dx from the CDC, the ratio of the energy deposited in the ECL and the momentum measured by the SVD and the CDC, the shower shape in the ECL, ACC information and the position matching between the shower and the track. With the above selections, the muon (electron) identification efficiency is above 90% and the hadron fake rate is less than 4% (0.5%).

We reconstruct J/ψ mesons in the $\ell^+\ell^-$ decay channel ($\ell = e$ or μ) and include bremsstrahlung photons that are within 50 mrad of either the e^+ or e^- tracks [hereinafter denoted as $e^+e^-(\gamma)$]. The invariant mass of the J/ψ candidate is required to satisfy $3.00 \text{ GeV}/c^2 < M_{e^+e^-(\gamma)} < 3.13 \text{ GeV}/c^2$ or $3.06 \text{ GeV}/c^2 < M_{\mu^+\mu^-} < 3.13 \text{ GeV}/c^2$ (with a distinct lower value accounting for the residual bremsstrahlung in the electron mode). A mass- and vertex-constrained fit is performed to the selected J/ψ candidate to improve its momentum resolution. The J/ψ candidate is then combined with a $\pi^+\pi^-$ pair to form an $X(3872)(\psi')$ candidate whose mass must satisfy $3.82 \text{ GeV}/c^2 < M_{J/\psi\pi\pi} < 3.92 \text{ GeV}/c^2$ ($3.64 \text{ GeV}/c^2 < M_{J/\psi\pi\pi} < 3.74 \text{ GeV}/c^2$). The dipion mass must also satisfy $M_{\pi\pi} > M_{J/\psi\pi\pi} - (m_{J/\psi} + 0.2 \text{ GeV}/c^2)$, where $m_{J/\psi}$ is nominal mass. This criterion corresponds to $M_{\pi\pi} > 575(389) \text{ MeV}/c^2$ for the $X(3872)(\psi')$ mass region and reduces significantly the combinatorial background [4] while also flattening the background shape distribution in $M_{J/\psi\pi\pi}$. To suppress the background from $e^+e^- \rightarrow q\bar{q}$ (where $q = u, d, s, c$) continuum events, we require $R_2 < 0.4$, where R_2 is the ratio of the second- to zeroth-order Fox-Wolfram moments [23].

To reconstruct a neutral (charged) B meson candidate, a $K^+\pi^-$ ($K_S^0\pi^+$) candidate is combined with the $X(3872)$ or ψ' candidate. We select B candidates using two kinematic variables: the energy difference $\Delta E = E_B - E_{\text{beam}}$ and the beam-energy constrained mass $M_{\text{bc}} = (\sqrt{E_{\text{beam}}^2 - p_B^2}/c^2)$, where E_{beam} is the beam energy and E_B and p_B are the energy and magnitude of momentum, respectively, of the candidate B meson, all calculated in the e^+e^- center-of-mass (CM) frame. Only B candidates having $M_{\text{bc}} > 5.27 \text{ GeV}/c^2$ and $|\Delta E| < 0.1 \text{ GeV}$ are retained for further analysis. After all selection criteria, approximately 35% of events have multiple B candidates. For an event with more than one B candidate, we select the candidate having the smallest value of

$$\chi^2 = \frac{(M_{\text{bc}} - 5.2792 \text{ GeV}/c^2)^2}{\sigma_{M_{\text{bc}}}^2} + \frac{\chi_B^2}{ndf}, \quad (1)$$

where $\sigma_{M_{\text{bc}}}$ is the M_{bc} resolution (estimated to be $2.925 \text{ MeV}/c^2$ from a fit to $B^0 \rightarrow \psi' K^+\pi^-$ events), χ_B^2 is the quality of the vertex fit of all charged tracks (excluding

the K_S^0 daughters), $ndf = (2N - 3)$ in this fit and N is the number of fitted tracks. The correct candidate is selected in about 60% of the $B \rightarrow X(3872)K\pi$ events with multiple entries.

To extract the signal yield of $B \rightarrow X(3872)(\rightarrow J/\psi\pi^+\pi^-)K\pi$, we perform a two-dimensional (2D) unbinned extended maximum likelihood fit to the ΔE and $M_{J/\psi\pi\pi}$ distributions. For the signal, the ΔE distribution is parametrized by the sum of a Crystal Ball [24] and a Gaussian function while the $M_{J/\psi\pi\pi}$ distribution is modeled using the sum of two Gaussians having a common mean. The 2D probability distribution function (PDF) is a product of the individual one-dimensional PDFs, as no sizable correlation is found.

The main background contribution in $B \rightarrow (J/\psi\pi^+\pi^-)K\pi$ is expected to arise from inclusive B decays to J/ψ , which is confirmed by the low background found in the J/ψ mass sidebands in the data. To study this background, we use a large Monte Carlo sample of $B \rightarrow J/\psi X$ events corresponding to 100 times the integrated luminosity of the data sample, and we find that few backgrounds are peaking in the $M_{J/\psi\pi\pi}$ distribution (nonpeaking in the ΔE distribution) and vice versa. The remaining backgrounds are combinatorial in nature and are flat in both distributions. This background is parametrized by first-order Chebyshev polynomial.

For the $B^0 \rightarrow X(3872)K^+\pi^-$ decay mode, a 2D fit is performed. The mean and resolution of $M_{J/\psi\pi\pi}$ and ΔE are fixed for the $X(3872)$ region from signal MC samples after being rescaled from the results of the $B^0 \rightarrow \psi'K^+\pi^-$ decay mode. Further, we correct the mean of a Gaussian function for the $M_{J/\psi\pi\pi}$ distribution because of a difference in the shift of the ψ' and $X(3872)$ reconstructed and generated masses as seen in MC samples. The tail parameters, α and n of the Crystal Ball (CB) function, and the ratios of the CB's area and width to the corresponding quantities of the Gaussian component are fixed according to the signal MC simulation. The peaking components can be divided into two categories: the one peaking in $M_{J/\psi\pi\pi}$ but nonpeaking in ΔE that comes from the $B \rightarrow X(3872)X'$ decays where the $X(3872)$ decays in $J/\psi\pi^+\pi^-$ (here X' can be any particle), and the other peaking in ΔE but nonpeaking in $M_{J/\psi\pi\pi}$ which comes from a B with the same final state where $J/\psi\pi^+\pi^-$ is not from a $X(3872)$. The peaking background in $\Delta E(M_{J/\psi\pi\pi})$ is found to have the same resolution as that of the signal, so the PDF is chosen to be the same as the signal PDF, while the nonpeaking background in the other dimension is parametrized with a first-order Chebyshev polynomial. Parameters (slopes) of the background PDFs, which are of nonpeaking or combinatorial nature, are allowed to vary in the fit. The fits are validated on full simulated experiments and no significant bias is seen. Figure 1 (top) shows the signal-enhanced projection plots for the $B^0 \rightarrow X(3872)(K^+\pi^-)$ decay

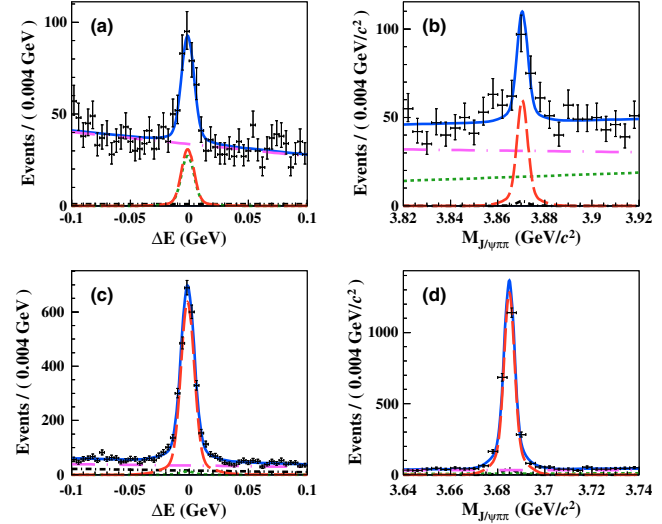


FIG. 1 (color online). Projections of the $(\Delta E, M_{J/\psi\pi\pi})$ fit for the $B^0 \rightarrow X(3872)(\rightarrow J/\psi\pi^+\pi^-)K^+\pi^-$ decay mode (top) and the $B^0 \rightarrow \psi'(\rightarrow J/\psi\pi^+\pi^-)K^+\pi^-$ decay mode (bottom): (a) ΔE distribution for $3.860 \text{ GeV}/c^2 < M_{J/\psi\pi\pi} < 3.881 \text{ GeV}/c^2$, (b) $M_{J/\psi\pi\pi}$ distribution for $-11 \text{ MeV} < \Delta E < 8 \text{ MeV}$, (c) ΔE distribution for $3.675 \text{ GeV}/c^2 < M_{J/\psi\pi\pi} < 3.695 \text{ GeV}/c^2$, and (d) $M_{J/\psi\pi\pi}$ distribution for $-11 \text{ MeV} < \Delta E < 8 \text{ MeV}$. The curves show the signal (red long-dashed curve) and the background components (black dash-dotted line for the component peaking in $M_{J/\psi\pi\pi}$ but nonpeaking in ΔE , green dashed line for the one peaking in ΔE but nonpeaking in $M_{J/\psi\pi\pi}$, and magenta long dash-dotted line for combinatorial background) as well as the overall fit (blue solid curve).

mode. The result of the fit and branching fractions derived are listed in Table I. We find a clear signal for $B^0 \rightarrow X(3872)K^+\pi^-$ of 116 ± 19 , signal events corresponding to a significance [25] (including systematic uncertainties related to the signal yield as mentioned in Table II) of 7.0 standard deviations (σ), and measure the product of branching fractions to be $\mathcal{B}(B^0 \rightarrow X(3872)K^+\pi^-) \times \mathcal{B}(X(3872) \rightarrow J/\psi\pi^+\pi^-) = (7.9 \pm 1.3(\text{stat}) \pm 0.4(\text{syst})) \times 10^{-6}$. The efficiency used for estimating the branching fraction is calculated from the individual efficiencies and the fractions of the different components obtained in the $(K^+\pi^-)$ mass, as explained below. The statistical significance is estimated using the value of $\sqrt{-2 \ln(\mathcal{L}_0/\mathcal{L}_{\text{max}})}$ where $\mathcal{L}_{\text{max}}(\mathcal{L}_0)$ denotes the likelihood value when the yield is allowed to vary (fixed to zero).

The above fit is validated on the calibration mode $B^0 \rightarrow \psi'K^+\pi^-$. In contrast to the $X(3872)$ mass region, the mean and resolution in both distributions ($M_{J/\psi\pi\pi}$ and ΔE) are allowed to vary in the fit. Figure 1 (bottom) shows the signal-enhanced projection plots for the $B^0 \rightarrow \psi'(K^+\pi^-)$ decay mode. We measure the branching fraction to be $\mathcal{B}(B^0 \rightarrow \psi'K^+\pi^-) = (5.79 \pm 0.14(\text{stat})) \times 10^{-4}$, consistent with an independent Belle result based on a Dalitz-plot analysis [26].

TABLE I. Signal yield (Y) from the fit, weighted efficiency (ϵ) after particle-identification correction, significance (Σ) and measured \mathcal{B} for $B^0 \rightarrow X(3872)K^+\pi^-$ and $B^+ \rightarrow X(3872)K^0\pi^+$. The first (second) uncertainty represents a statistical (systematic) contribution.

Decay mode	Y	ϵ (%)	$\Sigma(\sigma)$	$\mathcal{B}(B \rightarrow X(3872)K\pi) \times \mathcal{B}(X(3872) \rightarrow J/\psi\pi^+\pi^-)$
$B^0 \rightarrow X(3872)K^+\pi^-$	116 ± 19	15.99	7.0	$(7.9 \pm 1.3 \pm 0.4) \times 10^{-6}$
$B^+ \rightarrow X(3872)K^0\pi^+$	35 ± 10	10.31	3.7	$(10.6 \pm 3.0 \pm 0.9) \times 10^{-6}$

Further, to determine the contribution of the $K^*(892)$ and other intermediate states, we perform a 2D fit to ΔE and $M_{J/\psi\pi\pi}$ in each bin of $M_{K\pi}$ (0.1 GeV/ c^2 wide bins of $M_{K\pi}$ in the range [0.62, 1.42] GeV/ c^2), which provides a background-subtracted $M_{K\pi}$ signal distribution. All parameters of the signal PDFs for $M_{J/\psi\pi\pi}$ and ΔE distributions are fixed from the previous 2D fit to all events. We perform a χ^2 fit to the $M_{K\pi}$ distribution using $K^*(892)^0$ and $(K^+\pi^-)_{\text{NR}}$ components, which are histogram PDFs obtained from MC samples. Note that the $B^0 \rightarrow X(3872)K_2^*(1430)^0$ decay is kinematically suppressed. We do not consider the interference between the $K^*(892)$ and nonresonant component since the number of candidates is not large enough to make a full amplitude analysis. The resulting fit result is shown in Fig. 2(a). We obtain $38 \pm 14(82 \pm 21)$ signal events for the $B^0 \rightarrow X(3872)K^*(892)^0(B^0 \rightarrow X(3872)(K^+\pi^-)_{\text{NR}})$ decay mode, whose sum is consistent with the total yield obtained from the global fit. This corresponds to a 3.0σ significance (including systematic uncertainties related to the signal yield) for the $B^0 \rightarrow X(3872)(\rightarrow J/\psi\pi^+\pi^-)K^*(892)^0$ decay mode, and a product of branching fractions of $\mathcal{B}(B^0 \rightarrow X(3872)K^*(892)^0) \times \mathcal{B}(X(3872) \rightarrow J/\psi\pi^+\pi^-) = (4.0 \pm 1.5(\text{stat}) \pm 0.3(\text{syst})) \times 10^{-6}$. The ratio of branching fractions is

$$\frac{\mathcal{B}(B^0 \rightarrow X(3872)K^*(892)^0) \times \mathcal{B}(K^*(892)^0 \rightarrow K^+\pi^-)}{\mathcal{B}(B^0 \rightarrow X(3872)K^+\pi^-)} = 0.34 \pm 0.09(\text{stat}) \pm 0.02(\text{syst}). \quad (2)$$

TABLE II. Summary of the systematic uncertainties in percent.

	$X(3872)$	$X(3872)$
Source	$K^+\pi^-$	$K^0\pi^+$
Lepton ID	3.4	3.4
Kaon ID	1.1	...
Pion ID	2.5	3.2
PDF modeling	+1.8 -1.3	+4.2 -4.9
Tracking efficiency	2.1	2.5
K_S^0 reconstruction	...	0.7
$N_{B\bar{B}}$	1.4	1.4
Secondary \mathcal{B}	0.4	0.4
Efficiency	0.6	1.0
Fit bias	0.6	3.1
Total	5.4	8.0

In the above ratio, all systematic uncertainties cancel except those from the PDF model, fit bias and efficiency variation over the Dalitz distribution. We generate pseudoexperiments to estimate the significance of the χ^2 fit.

The $B^0 \rightarrow \psi'K^+\pi^-$ mode is analyzed with the same procedure, with 0.051 GeV/ c^2 wide bins, due to the copious yield, and in the $M_{K\pi}$ range [0.600, 1.569] GeV/ c^2 . We perform a χ^2 fit to the obtained $M_{K\pi}$ signal distribution again to extract the contributions of the $K\pi$ nonresonant and resonant components. For this purpose, we use histogram PDFs obtained from MC samples of several possible components of the $(K^+\pi^-)$ system: $K^*(892)^0$, $K_2^*(1430)^0$ and nonresonant $K^+\pi^-((K^+\pi^-)_{\text{NR}})$; in the last case, $B^0 \rightarrow \psi'(K^+\pi^-)_{\text{NR}}$ is generated uniformly in phase space. The fit result is shown in Fig. 2(b). The $K^*(892)$ dominates and we measure $\mathcal{B}(B^0 \rightarrow \psi'K^*(892)^0) = (5.88 \pm 0.18(\text{stat})) \times 10^{-4}$, which is consistent with the world average [3].

In contrast to $B^0 \rightarrow \psi'(K^+\pi^-)$ [where the ratio of branching fractions is $0.68 \pm 0.01(\text{stat})$], $B^0 \rightarrow X(3872)K^*(892)^0$ does not dominate in the $B^0 \rightarrow X(3872)K^+\pi^-$.

We also investigate the decays $B^+ \rightarrow X(3872)(\rightarrow J/\psi\pi^+\pi^-)(K^0\pi^+)$. The PDFs of ΔE and $M_{J/\psi\pi\pi}$ are the same as those for the neutral B meson decay mode. The projections of the 2D fit for $B^+ \rightarrow X(3872)(\rightarrow J/\psi\pi^+\pi^-)(K^0\pi^+)$ in the signal-enhanced regions are

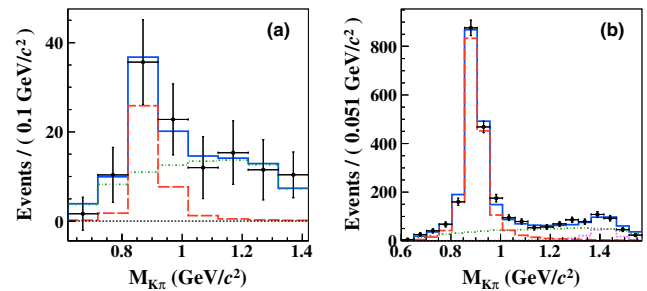


FIG. 2 (color online). Fit to the background-subtracted $M_{K\pi}$ distribution: (a) for the $B^0 \rightarrow X(3872)(K^+\pi^-)$ decay mode, the curves show the $B^0 \rightarrow X(3872)K^*(892)^0$ (red long-dashed lines), $B^0 \rightarrow X(3872)(K^+\pi^-)_{\text{NR}}$ (green dot-dashed lines), as well as the overall fit (blue solid lines). (b) for the $B^0 \rightarrow \psi'(K^+\pi^-)$ decay mode, the curves show the $B^0 \rightarrow \psi'K^*(892)^0$ (red long-dashed lines), $B^0 \rightarrow \psi'(K^+\pi^-)_{\text{NR}}$ (green dot-dashed lines), $B^0 \rightarrow \psi'K_2^*(1430)^0$ (magenta dashed lines) as well as the overall fit (blue solid lines).

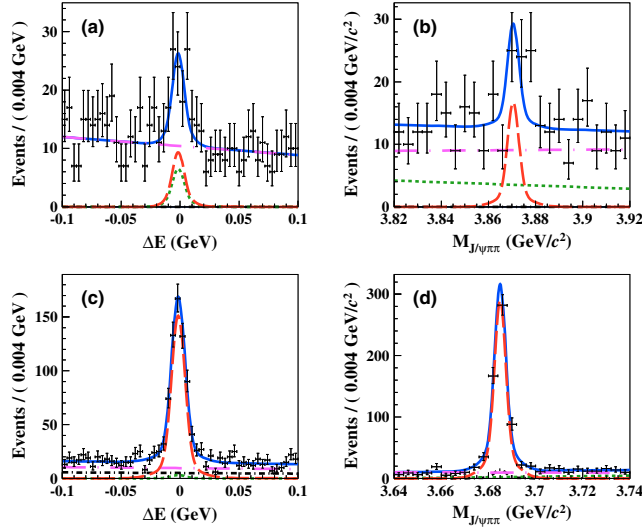


FIG. 3 (color online). Projections of the $(\Delta E, M_{J/\psi\pi\pi})$ fit for the $B^\pm \rightarrow X(3872)(\rightarrow J/\psi\pi^+\pi^-)K_S^0\pi^\pm$ decay mode (top) and for the $B^\pm \rightarrow \psi'(\rightarrow J/\psi\pi^+\pi^-)K_S^0\pi^\pm$ decay mode (bottom): (a) ΔE distribution for $3.859 \text{ GeV}/c^2 < M_{J/\psi\pi\pi} < 3.882 \text{ GeV}/c^2$, (b) $M_{J/\psi\pi\pi}$ distribution for $-11 \text{ MeV} < \Delta E < 9 \text{ MeV}$, (c) ΔE distribution for $3.675 \text{ GeV}/c^2 < M_{J/\psi\pi\pi} < 3.695 \text{ GeV}/c^2$, and (d) $M_{J/\psi\pi\pi}$ distribution for $-11 \text{ MeV} < \Delta E < 9 \text{ MeV}$. The curves show the signal (red long-dashed curves); and the background components (black dash-dotted curves for the component peaking in $M_{J/\psi\pi\pi}$ but nonpeaking in ΔE , green dashed lines for the one peaking in ΔE but nonpeaking in $M_{J/\psi\pi\pi}$, and magenta long dash-dotted lines for combinatorial background) as well as the overall fit (blue solid curves).

shown in Figs. 3(a) and 3(b). We find 35 ± 10 events for the $B^+ \rightarrow X(3872)(\rightarrow J/\psi\pi^+\pi^-)(K^0\pi^+)$ decay mode, corresponding to a 3.7σ significance (including systematic uncertainties). The product of branching fractions is $\mathcal{B}(B^+ \rightarrow X(3872)K^0\pi^+) \times \mathcal{B}(X(3872) \rightarrow J/\psi\pi^+\pi^-) = (10.6 \pm 3.0(\text{stat}) \pm 0.9(\text{syst})) \times 10^{-6}$. The above fit is validated for the ψ' mass region. The projections of the 2D fit for $B^+ \rightarrow \psi'(\rightarrow J/\psi\pi^+\pi^-)(K^0\pi^+)$ in the signal-enhanced regions are shown in Figs. 3(c) and 3(d). The branching fraction for $B^+ \rightarrow \psi'(\rightarrow J/\psi\pi^+\pi^-)(K^0\pi^+)$ is $(6.00 \pm 0.28(\text{stat})) \times 10^{-4}$, while the world average of this quantity is $(5.88 \pm 0.34) \times 10^{-4}$.

Equal production of neutral and charged B meson pairs in the $\Upsilon(4S)$ decay is assumed. Secondary branching fractions used for calculation of \mathcal{B} are taken from Ref. [3]. Systematic uncertainties are summarized in Tables II and III. A correction for small differences in the signal detection efficiency between signal MC events and data due to lepton, kaon and pion identification differences is applied; samples of $J/\psi \rightarrow \ell^+\ell^-$ and $D^{*+} \rightarrow D^0(\rightarrow K^-\pi^+)\pi^+$ decays are used to estimate this correction. The uncertainties on these corrections are included in the systematic error. The uncertainty due to the fitting model is obtained by varying all fixed parameters by $\pm 1\sigma$

TABLE III. Summary of systematic uncertainties (in percent) used for the $M_{K\pi}$ background-subtracted fit in $B^0 \rightarrow X(3872)K^+\pi^-$.

Source	$X(3872)K^*(892)^0$
Lepton ID	3.4
Kaon ID	1.1
Pion ID	2.6
PDF modeling	+1.5 -1.4
Tracking efficiency	2.1
$N_{B\bar{B}}$	1.4
Secondary B	0.4
MC statistics	0.2
Fit bias	4.6
Total	7.0

and considering the corresponding change in the yield as the systematic error. The uncertainties due to tracking efficiency, K_S^0 reconstruction and $N_{B\bar{B}}$ are estimated to be 0.35% per track, 0.7% and 1.4%, respectively. The systematic uncertainty due to secondary branching fractions is included. The systematic uncertainty for the efficiency arises from the limited MC statistics, and the efficiency variation over the Dalitz distribution is also considered. Small biases in the fitting procedure, estimated in the ensemble study, are also considered as a source of systematic uncertainty. For this study we perform a fit to 100 pseudoexperiments after embedding signal events obtained from MC samples to each inclusive MC sample. All the above stated systematic uncertainties are added in quadrature and result in a total systematic uncertainty of 5.4%, 8.0%, 7.0% for $B^0 \rightarrow X(3872)K^+\pi^-$, $B^+ \rightarrow X(3872)K_S^0\pi^+$ and $B^0 \rightarrow X(3872)K^*(892)^0$, respectively.

In summary, we report the first observation of the $X(3872)$ in the decay $B^0 \rightarrow X(3872)K^+\pi^-$, $X(3872) \rightarrow J/\psi\pi^+\pi^-$. The result for the $X(3872)$, where $B^0 \rightarrow X(3872)K^*(892)^0$ does not dominate the $B^0 \rightarrow X(3872)(K^+\pi^-)$ decay, is in marked contrast to the ψ' case. We have checked for a structure in the $X(3872)\pi$ and $X(3872)K$ invariant masses and found no evident peaks. We measure $\mathcal{B}(B^0 \rightarrow X(3872)(K^+\pi^-)) \times \mathcal{B}(X(3872) \rightarrow J/\psi\pi^+\pi^-) = (7.9 \pm 1.3(\text{stat}) \pm 0.4(\text{syst})) \times 10^{-6}$ and $\mathcal{B}(B^+ \rightarrow X(3872)K^0\pi^+) \times \mathcal{B}(X(3872) \rightarrow J/\psi\pi^+\pi^-) = (10.6 \pm 3.0(\text{stat}) \pm 0.9(\text{syst})) \times 10^{-6}$.

We thank the KEKB group for the excellent operation of the accelerator; the KEK cryogenics group for the efficient operation of the solenoid; and the KEK computer group, the National Institute of Informatics, and the PNNL/EMSL computing group for valuable computing and SINET4 network support. We acknowledge support from the Ministry of Education, Culture, Sports, Science, and Technology (MEXT) of Japan, the Japan Society for the Promotion of Science (JSPS), and the Tau-Lepton Physics Research Center of Nagoya University; the Australian

Research Council and the Australian Department of Industry, Innovation, Science and Research; Austrian Science Fund under Grants No. P 22742-N16 and No. P 26794-N20; the National Natural Science Foundation of China under Contracts No. 10575109, No. 10775142, No. 10875115, No. 11175187, and No. 11475187; the Ministry of Education, Youth and Sports of the Czech Republic under Contract No. LG14034; the Carl Zeiss Foundation, the Deutsche Forschungsgemeinschaft and the VolkswagenStiftung; the Department of Science and Technology of India; the Istituto Nazionale di Fisica Nucleare of Italy; National Research Foundation (NRF) of Korea Grants No. 2011-0029457, No. 2012-0008143, No. 2012R1A1A2008330, No. 2013R1A1A3007772, No. 2014R1A2A2A01005286, No. 2014R1A2A2A01002734, No. 2014R1A1A2006456; the Basic Research Lab program under NRF Grant No. KRF-2011-0020333, No. KRF-2011-0021196, Center for Korean J-PARC

Users, No. NRF-2013K1A3A7A06056592; the Brain Korea 21-Plus program and the Global Science Experimental Data Hub Center of the Korea Institute of Science and Technology Information; the Polish Ministry of Science and Higher Education and the National Science Center; the Ministry of Education and Science of the Russian Federation and the Russian Foundation for Basic Research; the Slovenian Research Agency; the Basque Foundation for Science (IKERBASQUE) and the Euskal Herriko Unibertsitatea (UPV/EHU) under program UFI 11/55 (Spain); the Swiss National Science Foundation; the National Science Council and the Ministry of Education of Taiwan; and the U.S. Department of Energy and the National Science Foundation. This work is supported by a Grant-in-Aid from MEXT for Science Research in a Priority Area (“New Development of Flavor Physics”) and from JSPS for Creative Scientific Research (“Evolution of Tau-lepton Physics”).

-
- [1] S. K. Choi *et al.* (Belle Collaboration), *Phys. Rev. Lett.* **91**, 262001 (2003).
 - [2] Charge-conjugate decays are included unless explicitly stated otherwise.
 - [3] K. A. Olive *et al.* (Particle Data Group), *Chin. Phys. C* **38**, 090001 (2014).
 - [4] S. K. Choi *et al.* (Belle Collaboration), *Phys. Rev. D* **84**, 052004 (2011).
 - [5] R. Aaij *et al.* (LHCb Collaboration), *Phys. Rev. Lett.* **110**, 222001 (2013).
 - [6] V. Bhardwaj *et al.* (Belle Collaboration), *Phys. Rev. Lett.* **107**, 091803 (2011).
 - [7] R. Aaij *et al.* (LHCb Collaboration), *Nucl. Phys. B* **886**, 665 (2014).
 - [8] P. del Amo Sanchez *et al.* (BABAR Collaboration), *Phys. Rev. D* **82**, 011101(R) (2010).
 - [9] T. Aushev *et al.* (Belle Collaboration), *Phys. Rev. D* **81**, 031103(R) (2010).
 - [10] B. Aubert *et al.* (BABAR Collaboration), *Phys. Rev. D* **77**, 011102(R) (2008).
 - [11] E. S. Swanson, *Phys. Lett. B* **598**, 197 (2004); E. S. Swanson, *Phys. Rep.* **429**, 243 (2006).
 - [12] M. Suzuki, *Phys. Rev. D* **72**, 114013 (2005).
 - [13] L. Maiani, F. Piccinini, A. D. Polosa, and V. Riquer, *Phys. Rev. D* **71**, 014028 (2005).
 - [14] B. Aubert *et al.* (BABAR Collaboration), *Phys. Rev. D* **71**, 031501 (2005).
 - [15] T. Iwashita *et al.* (Belle Collaboration), *Prog. Theor. Exp. Phys.* **2014**, 43C01 (2014).
 - [16] V. Bhardwaj *et al.* (Belle Collaboration), *Phys. Rev. Lett.* **111**, 032001 (2013).
 - [17] A. Abashian *et al.* (Belle Collaboration), *Nucl. Instrum. Methods Phys. Res., Sect. A* **479**, 117 (2002); also see detector section in J. Brodzicka *et al.*, *Prog. Theor. Exp. Phys.* **2012**, 4D001 (2012).
 - [18] S. Kurokawa and E. Kikutani, *Nucl. Instrum. Methods Phys. Res., Sect. A* **499**, 1 (2003), and other papers included in this volume; T. Abe *et al.*, *Prog. Theor. Exp. Phys.* **2013**, 03A001 (2013), and following articles up to 03A011.
 - [19] D. J. Lange, *Nucl. Instrum. Methods Phys. Res., Sect. A* **462**, 152 (2001).
 - [20] E. Barberio and Z. Wąs, *Comput. Phys. Commun.* **79**, 291 (1994); P. Golonka and Z. Wąs, *Eur. Phys. J. C* **45**, 97 (2006); **50**, 53 (2007).
 - [21] R. Brun *et al.*, GEANT3.21, CERN Report No. DD/EE/84-1, 1984.
 - [22] K.-F. Chen *et al.* (Belle Collaboration), *Phys. Rev. D* **72**, 012004 (2005).
 - [23] G. C. Fox and S. Wolfram, *Phys. Rev. Lett.* **41**, 1581 (1978).
 - [24] T. Skwarnicki, Ph.D. thesis, Institute for Nuclear Physics, Krakow, 1986; , DESY, Internal Report No. DESY F31-86-02, 1986.
 - [25] R. D. Cousins and V. L. Highland, *Nucl. Instrum. Methods Phys. Res., Sect. A* **320**, 331 (1992).
 - [26] K. Chilikin *et al.* (Belle Collaboration), *Phys. Rev. D* **88**, 074026 (2013).